Journal Name

ARTICLE

Dinucleating Schiff base ligand in Zn/4f coordination chemistry: Synthetic challenges and catalytic activity evaluation

Stavroula I. Sampani,[a] Sidonie Aubert,[†,b] Martin Cattoen,[†,b] Kieran Griffiths,[a] Alaa Abdul-Sada,[a] Geoffrey R. Akien,[c] Graham J. Tizzard,[d] Simon J. Coles,[d] Stellios Arseniyadis,[b,*] George E. Kostakis[a,*]

Four Zn/4f polynuclear coordination clusters (PCCs) formulated as $[Zn^{II}_2Dy^{III}_2L_2(CO_3)_2(NO_3)_2]$ (**1**), $[Zn^{II}Y^{III}L(NO_3)_2(o\text{-van})(MeOH)]$ (MeOH) [**2** (MeOH)] and $[Zn^{II}Ln^{III}L(NO_3)_2Cl(EtOH)]$ where Ln is Dy (**3**) and Y (**4**) and where H_2L is the dinucleating Schiff base ligand N,N'-bis(3-methoxysalicylidene)cyclohexane-1,2-diamine and o-van is *ortho*-vanillin, were prepared and fully characterised for the first time. These air-stable heterometallic PCCs, obtained in high yields from commercially available materials, were shown to remain stable in solution in their dinuclear $[Zn^{II}Ln^{III}L]$ form. Their catalytic activity was evaluated in various catalytic transformations including the Friedel-Crafts alkylation of 2-acyl imidazoles with indoles.

Introduction

Coordination clusters (CCs)[1] have recently been the centre of intense scrutiny due to their fascinating magnetic[2–4] and luminescent properties[5,6] as well as the very diverse core topologies[7–11] they display. Remarkably, several well characterized or *in situ* formed homometallic[12–15] or heterometallic[16–19] CCs were found to promote organic transformations, whereas fewer examples of heterometallic 3d/4f CCs have been tested for their catalytic activity. These can be classified into two kinds. The first category incorporates *in-situ* generated catalysts from designed ligands and 3d/4f metal salts without prior characterisation of the pre-catalyst or postulated active species. These examples, were shown to promote a number of transformations including the *syn*-selective nitro-Mannich reaction,[20,21] the *anti*-selective asymmetric Henry reaction[22] and the asymmetric decarboxylative 1,4-addition of malonic acid half-thioesters.[23] Solution studies showed the existence of other $(3d)_x(4f)_x$ oligomers, where x ranges from 3 to 9, in the presence of protic solvents or additives.[20,21] In addition, tuning the 4f centre and the metal salt, led to a decrease in the efficacy of the corresponding catalyst.

The second group of 3d/4f CCs includes paradigms of well-characterised pre-catalyst or postulated active species.[24–33] The advantage of the isolation and use of well-defined species compared to the former set is the possibility to extract

mechanistic information by performing controlled experiments and thus shed light in the catalytic nature of the 3d/4f PCCs. Moreover, this approach allows to fine tune the reaction conditions (*i.e.* optimize the catalyst loadings <0.5 mol%). For example the isoskeletal tetranuclear Co^{II}_3Ln CCs were introduced as a new springboard water oxidation catalyst,[24] whereas heptanuclear 3d–4f helicates show high catalytic activity for the coupling of CO_2 and epoxides to obtain cyclic carbonates with a wide substrate scope at ambient temperature and pressure.[33] Our group has reported the synthesis and characterization of a series of isoskeletal "butterfly" shaped tetranuclear $[3d^{II}_2 4f^{III}_2 L_4]^{2+}$ (3d = Ni, Co, Cu, Zn, 4f = Y, Sm, Dy, Gd, Sm) CCs, in which the coordination spheres of the 3d and the 4f ions are not fully saturated, and their use in a series of organic transformations.[26–29,32] This catalytic library showcased cooperative catalytic behaviour, while variation of the 4f centre permitted the extraction of useful mechanistic information.[29] However, our efforts to obtain isoskeletal derivatives altering the counter ion and/or the lanthanide source yielded in the isolation of unexpected products with variant formulations, which could be attributed to several parameters including the pH of the reaction and the coordination ability of the anion and/or the ionic radii of the lanthanide element.[28]

Taking all these into account and considering the successful use in catalysis[20,21] of the *in-situ* formed 3d/4f CCs built from a dinucleating Schiff base ligand, we initiated a project to investigate the synthesis and characterization of dinuclear Zn/4f CCs and evaluate their catalytic activity in various reactions including the Friedel-Crafts alkylation of acylimidazole-derived enones. We have chosen to use the dinucleating Schiff base N,N'-bis(3-methoxysalicylidene) cyclohexane-1,2-diamine (H_2L, Scheme 1) as the ligand and Dy or Y as the 4f source. Y^{III} has a size and Lewis acidity similar to Ho^{III} and Dy^{III}, and its use permits characterization in solution. We prepared the CCs formulated as $[Zn^{II}_2Dy^{III}_2L_2(CO_3)_2$ $(NO_3)_2]$ (**1**), $[Zn^{II}Y^{III}_2L(NO_3)_2(o\text{-}$

van)(MeOH)](MeOH) [**2** (MeOH)]) and [$Zn^{II}Ln^{III}L(NO_3)_2Cl$ (EtOH)] where Ln is Dy (**3**) and Y (**4**). All compounds were subjected to ESI-MS solution studies, whereas the stability of the diamagnetic Zn/Y analogues was investigated with ^1H and ^{89}Y NMR before being evaluated for their catalytic activity. We report here the results of our endeavour.

Experimental

Materials. Chemicals (reagent grade) were purchased from Sigma Aldrich, Fluorochem, TCI and Alfa Aesar. All experiments were performed under aerobic conditions using materials and solvents as received.

Instrumentation. IR spectra were recorded over the range of 4000-650 cm^{-1} on a Perkin Elmer Spectrum One FT-IR spectrometer fitted with a UATR polarization accessory. ESI-MS data were obtained on Bruker Daltonics Fourier transform ion cyclotron (FTICR-MS) while the EI (at 70 eV) were obtained using Fissions instrument VG Autospec. NMR spectra were measured on a Varian VNMRS solution-state spectrometer (Bruker BioSpin, Rheinstetten, Germany) at 500 MHz at 30 °C using residual isotopic solvent (DMSO-d6, δ_H = 2.50 ppm) as an internal chemical shift reference. ^1H DOSY (ledbpgp2s), ^{15}N-HMBC and ^{89}Y-HMQC spectra were acquired at 298.0 K on a Bruker Avance III 400 instrument (Bruker BioSpin) equipped with a broadband observe probe (BBO). Chemical shifts are quoted in ppm. Coupling constants (*J*) are recorded in Hz. In contrast to earlier work,[23,26] we were unable to observe any ^1H-^{89}Y HMBC correlations, perhaps due to exchange broadening.

Synthesis of H_2L. *o*-Vanillin (2.0 g, 2.6 x 10^{-2} mol) and 1,2-diaminocyclohexane (0.74 g, 1.3 x 10^{-2} mol) were refluxed in MeOH (40 mL) for 2 h. The resulting clear yellow solution was then concentrated under reduced pressure and the crude residue was purified by flash column chromatography over silica gel (Hexanes/EtOAc: 80:20) to form the desired compound.

Synthesis of the metallo-ligand ZnL. Following a previously reported procedure,[34] H_2L (0.77 g, 2.0 mmol) was suspended in EtOH (20 mL) and stirred under reflux for 10 min. An aqueous solution (5 mL) of $Zn^{II}(OAc)_2\cdot 4H_2O$ (0.44 g, 2.0 mmol) was then added and the resulting mixture was refluxed for 2 h, time after which a pale yellow precipitate formed and was separated by filtration. The latter was washed with MeOH (3 x 20 mL) and Et_2O (2 x 15 mL) to yield Zn-L in 89% yield.

Synthetic Protocol for the synthesis of $Zn^{II}-Ln^{III}$ PCCs (1-4). [$Zn^{II}_2Dy^{III}_2L_2(CO_3)_2(NO_3)_2$] (**1**) and [$Zn^{II}Y^{III}L(NO_3)_2$(o-van)(MeOH)] (MeOH) [**2** (MeOH)] were prepared following the similar synthetic pathway. The metallo-ligand ZnL (44 mg, 0.1 mmol) was suspended in MeOH (20 mL) and stirred for 5 min. $Ln(NO_3)_3\cdot 5H_2O$ (0.1 mmol) was subsequently added and the reaction mixture was stirred for an additional hour. The resulting clear yellow solution was eventually filtered and left for slow evaporation. After 9-15 days, small colourless needles suitable for X-Ray diffraction were formed (yield 49% for **1** and 35% for **2**). CHN **1** [$Zn^{II}_2Dy^{III}_2L_2(NO_3)_2(CO_3)_2$] observed: C-37.56%, H-3.38%, N-5.81%, expected: C-37.82%, H-3.31%,

N-5.70%. CHN **2** [$Zn^{II}Y^{III}L(NO_3)_2$(o-van)(MeOH)] (MeOH) [**2** (MeOH)] observed: C-44.41%, H-4.28%, N-6.80%, expected: C-43.98%, H-4.50%, N-6.41%.

[$Zn^{II}Ln^{III}L(NO_3)_2Cl(EtOH)$], where Ln is Dy^{III} (**3**) and Y^{III} (**4**), were prepared following a different synthetic pathway in comparison to **1** and **2**. After suspending H_2L (38 mg, 0.1 mmol) in EtOH (20 mL) and stirring for 5 min, $Ln(NO_3)_3\cdot 5H_2O$ (0.1 mmol) and $ZnCl_2$ (0.1 mmol) were added and stirring was continued for 1 h to form a clear yellow solution. The latter was filtered and left for slow evaporation. After 6-9 days, colourless crystalline blocks suitable for single X-Ray diffraction were collected and dried overnight (37-49% yield based on Ln^{III}). CHN **3** [$Zn^{II}Dy^{III}L(NO_3)_2Cl(EtOH)$] observed: C-35.18%, H-3.76%, N-6.84%, expected: C-35.42%, H-3.72%, N-6.88%. CHN **4** [$Zn^{II}Y^{III}L(NO_3)_2Cl(EtOH)$] observed: C-38.85%, H-4.13%, N-7.45%, expected: C-38.94%, H-4.18%, N-7.57%.

X-Ray Crystallography. Data for **2** (ω-scans) were obtained at the University of Sussex using an Agilent Xcalibur Eos Gemini Ultra diffractometer with CCD plate detector under a flow of nitrogen gas at 173(2) K. Data for **1, 3** and **4** were collected at the National Crystallography Service, University of Southampton[35] either a Rigaku FRE+ diffractometer equipped with a HG Saturn 724+ CCD detector (**1, 4**) or a Rigaku 007HF diffractometer equipped with a HyPix 6000 Hybrid Photon Counting (HPC) detector (**3**) under a flow of nitrogen gas at 100(2) K, processed with CrysAlisPro and solved by intrinsic phasing methods with SHELXT.[36] All crystal structures were then refined on Fo^2 by full-matrix least-squares refinements using SHELXL.[36] All non-H atoms were refined with anisotropic thermal parameters, and H-atoms were introduced at calculated positions and allowed to ride on their carrier atoms. Geometric/crystallographic calculations were performed using PLATON,[37] Olex2,[38] and WINGX[39] packages; graphics were prepared with Crystal Maker.[40] Crystallographic details are given in Table S1. CCDC 1820463-1820466

General procedure for the Friedel-Crafts alkylations and Michael additions. An oven-dried 10 mL vial was charged with a solution of the catalyst (0.025 mol/L in MeOH, 66.6 µL, 0.0017 mmol, 0.010 equiv.) and the solvent was evaporated to prevent any potential side reaction with MeOH. The catalyst was then dissolved in EtOAc (1.00 mL, C = 0.17 mol/L) and the α,β-unsaturated acyl imidazole **5** (25.0 mg, 0.17 mmol, 1.00 equiv.) was added along with the desired nucleophile **8** (0.18 mmol, 1.10 equiv.). The reaction mixture was then stirred at room temperature until complete conversion of the starting material (reaction monitored by TLC) and concentrated under reduced pressure to afford a crude residue, which was purified by flash column chromatography over silica gel.

Results and discussion

Synthetic issues. Prior to synthesis, we reviewed the literature and summarized two synthetic methodologies (Scheme 1 & Table 1).[30,34,41–48] The first incorporates the in situ blending of Zn, Ln sources and the ligand (Table 1, entries 1-3, 10), whereas the second, which is in favour, incorporates the stepwise

synthesis of the neutral ZnL unit, which in turn reacts with the corresponding Ln source (Table 4-9, 11, 12). The ligand indeed shows a dinucleating character binding to both 3d and 4f metal ions. In all the examples, L^{2-} is chelated to the Zn^{II} ion through the imino and the phenoxide groups (N_2O_2 pocket), whereas the Ln^{III} binds to the four O atoms from the two methoxides and the two phenoxides (OOOO pocket). To the best of our knowledge, only three examples of dinuclear Zn^{II}-Ln^{III} PCCs have been reported (Table 1, entries 1-3). It is worth pointing out that the use of different metal salts or lanthanides with smaller radii has significant impact in the motif of the final product. For example, the use of $Ln(OAc)_3$ and $Zn(OAc)_2$, resulted in di-, tri- and tetranuclear Zn^{II}/Ln^{III} CCs (Table 1, entries, 3, 5 and 10), whereas the use of a 1:1 mixture of $Ln(OAc)_3$ and ZnL yields the trinuclear $Zn^{II}_2Ln^{III}$ motif (Table 1, entries 5, and 8). Interestingly, the use of $LnCl_3$ and ZnL in 1:1 ratio led to the trinuclear $Zn^{II}_2Ln^{III}$ (Table 1, entries 4, 6, 7 and 9). Moreover, the use of co-ligands significant influences the formulation (Table 1, entries 7, 11, 12). All these notes showcase the importance of preparing stable and well-defined 3d/4f CC catalysts rather than generating them *in situ*.
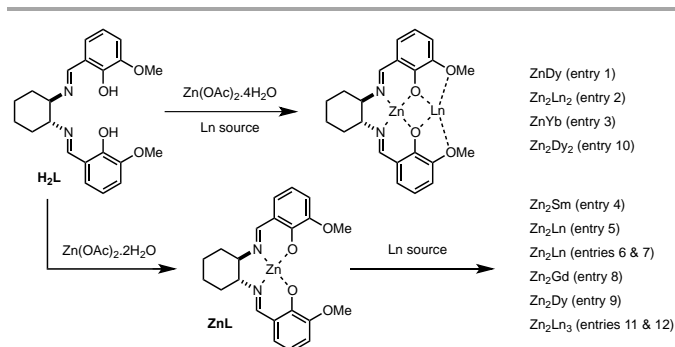
Scheme 1. The protonated form of the organic ligand used in this study and the different synthetic approaches reviewed up to now.

Our primary synthetic goal was the synthesis and characterization of the corresponding dinuclear "ZnLnLCl₃" and "ZnLnL(NO₃)₃" entities and having all the aforementioned notes in mind. We therefore decided to follow both synthetic strategies and discover their efficiency (Scheme 2). First, we isolated ZnL, which was subsequently reacted with $Dy(NO_3)_3$ or $Y(NO_3)_3$ in MeOH at room temperature. These reactions yielded large yellow block crystals in good yields corresponding to the tetranuclear $[Zn^{II}_2Dy^{III}_2L_2(CO_3)_2(NO_3)_2]$ (**1**) and the dinuclear $[Zn^{II}Y^{III}L(NO_3)_2$ (o-van)(MeOH)] (**2**) CCs. In the first case during crystallization, CO_2 fixation is observed which in turn is converted to CO_3^{2-}. A similar observation has been reported before.[41] Surprisingly, despite Y^{III} having similar ionic radii with Dy^{III}, the analogous reaction yields the dinuclear species **2**. In this case, as the crystallographic characterization indicates, the parent ligand (H_2L) partially dissociates to the starting materials (see ESI) and the oxophilic o-vanillin fulfils the vacant positions of coordination sphere of the Y^{III} centre. To confirm this result, the synthesis of **2** was repeated three times and three different crystallographic data sets confirmed the sole formation of **2**. To the best of our knowledge, this is the first report that such a

peculiar behaviour (Dy – CO_2 fixation, Y – ligand dissociation) is reported in a given specific 3d/4f synthetic system. We envisage that additional data are required to fully understand and thus rationalize this "atypical" behaviour. Moreover, the *in situ* reactions of H_2L and the nitrate salts of Zn and Dy or Y resulted in **1** and **2** in lower yields, showcasing the advantage of the stepwise over the *in situ* synthesis.

Table 1. Reported $Zn^{II}Ln^{III}$ CCs with H_2L ascended by nuclearity.

Entry	Formula	Ln^{III}	Conditions	Nuclearity	Ref
1	$[Zn^{II}Dy^{III}L(OAc)_2(NO_3)]\cdot MeOH$	Dy	H_2L:Dy(NO₃)₃.5H₂O: Zn(OAc)₂.4H₂O:2Et₃N MeOH/CH₃CN	2	46
2	$[Zn^{II}_2Ln^{III}_2L_2(4,4'\text{-bpe})(NO_3)_6]$	La, Nd, Yb Er, Gd	H_2L:Dy(NO₃)₃:Zn(OAc)₂.4H₂O MeCN	2	39
3	$[Zn^{II}Yb^{III}(OAc)_3L(H_2O)]$	Yb	H_2L:Dy(OAc)₃.xH₂O:Zn(OAc)₂.4H₂O EtOH	2	28
4	$[Sm^{III}(Zn^{II}L)_2Cl_2(H_2O)_2]\cdot PF_6$	Sm	ZnL:SmCl₃:1.5NH₄PF₆ H₂O/CH₂Cl₂	3	40
5	$[Zn^{II}_2Ln^{III}L(OAc)_2]\cdot OAc$	Nd, Yb Er, Gd	ZnL:Ln(OAc)₃ MeCN/MeOH	3	41
6	$[Zn^{II}_2Ln^{III}L_2(Cl)_3]$	Nd, Yb Er, Gd	ZnL:LnCl₃ MeCN/MeOH	3	42
7	$[Zn^{II}_2Ln^{III}L_2(MeOH)Cl\,(N_3)]$	La, Nd, Yb Er, Gd	ZnL:LnCl₃:3 NaN₃ MeCN	3	43
8	$[Zn^{II}_2Gd^{III}L_2(OAc)_2]PF_6\cdot$ MeOH·H₂O	Gd	ZnL:Gd(OAc)₃.4H₂O:1.5NH₄PF₆ MeOH	3	44
9	$[Zn^{II}_2Dy^{III}L_2Cl_3].2H_2O$	Dy	2ZnL:2DyCl₃.xH₂O:4,4'-bpe CH₃CN	3	44
10	$[Zn^{II}_2Dy^{III}_2L_2(OAc)_2(CO_3)_2]\cdot 10MeOH$	Dy	H_2L:Dy(ClO₄)₃:Zn(OAc)₂:3Et₃N MeOH/CH₂Cl₂	4	38
11	$[Zn^{II}_2Ln^{III}_3L_3Cl_2(\mu_2\text{-OH})\,(\mu_3\text{-OH})_2(N_3)_2]$	La, Nd, Yb Er, Gd	ZnL:LnCl₃:3NaN₃ MeCN	5	43
12	$[Zn^{II}_2Ln^{III}_3L_3Cl_2(\mu_2\text{-OH})(\mu_3\text{-OH})_2(N_3)_2]$	Nd, Yb, Er	ZnL:LnCl₃:3NaN₃ MeOH/MeCN	5	31
13	$[Zn^{II}_2Dy^{III}_2L_2(CO_3)_2(NO_3)_2]$	Dy	ZnL:Dy(NO₃)₂ MeOH	4	*this work*
14	$[Zn^{II}Y^{III}L(NO_3)_2(o\text{-van})_2(MeOH)]$	Y	ZnL:Y(NO₃)₂ MeOH	2	*this work*
15	$[Zn^{II}Ln^{III}L(NO_3)_2Cl(EtOH)]$	Y, Dy	H_2L:Ln(NO₃)₂:ZnCl₂ MeOH	2	*this work*

Both synthetic methodologies were involved towards the synthesis of the targeted "ZnLnLCl₃" entity, however in both cases the corresponding trinuclear Zn_2LnCl_3 CC is formed (Table 1, entry 9).[45,48] Then, our efforts focused on the possibility of isolating the hybrid Cl-NO₃ dinuclear derivative. Therefore, only in-situ reactions were performed.
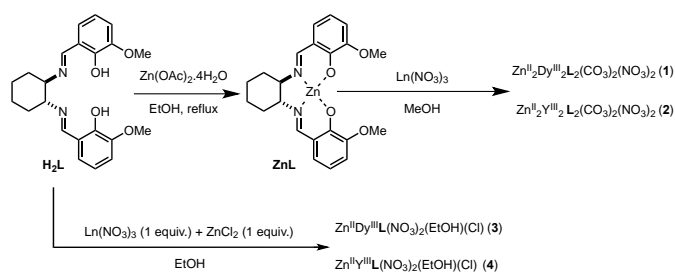
Scheme 2. A general synthetic overview for the synthesis of $Zn^{II}Ln^{III}$ PCCs **1-4**.

The blend of $Ln(NO_3)_3\cdot 6H_2O$, $ZnCl_2$ and H_2L in EtOH, reactions in MeOH produced bad quality crystalline material,

yielded after 4 days thin colourless needle-like crystals which were shown to possess a dinuclear configuration [$Zn^{II}Ln^{III}L(NO_3)_2Cl(EtOH)$]], where Ln is Dy (**3**) and Y (**4**) (49% and 61% yield for **3** and **4**, respectively). The analogous reactions of $LnCl_3 \cdot xH_2O$, $Zn(NO_3)_2$ $6H_2O$ and H_2L in EtOH, resulted in **3** (Dy) and **4** (Y) in lower yields (40% and 52%, respectively).

Molecular Structure and Crystallographic Descriptions. Compound **1** (Figure 1, a) crystallises in the monoclinic space group P2_1/c. The asymmetric units contains one Zn^{II} ion, one Dy^{III} ion, one doubly deprotonated organic ligand **L**, one carbonate and one nitrate molecule. The main core can be considered as two [$Zn^{II}Dy^{III}L(NO_3)(CO_3)$] moieties bridged by two carbonate groups. Each organic ligand is chelated to the Zn^{II} ion via the two imino N atoms and the two phenoxide O atoms to the Dy^{III} ion *via* the two methoxido and two phenoxide O atoms. The carbonate group bridges the two Dy^{III} ions *via* oxygen O4 and coordinates to Zn_2 and the nitrate group is chelated to the Dy^{III} ion. The distorted square pyramidal geometry (N_2O_3) of the Zn^{II} ion is fulfilled by the bridging carbonate group (Figure 1). The coordination number of the Dy^{III} is nine and the coordination geometry can be best described as pentagonal bipyramid (7+2) (considering the two O atoms from the chelated NO_3 and CO_3 units as only one), whereas analysis with SHAPE software[49] suggests a capped square antiprismatic geometry (Table S2). There is one Zn^{II}-Dy^{III} distance at 3.377(2) Å and one Dy^{III}-Dy^{III} distance at 4.052 Å. Compound **2** (Figure 1, b) crystallizes in the triclinic *P*-1 space group. The asymmetric unit contains one Zn^{II} ion, one Y^{III} ion, one doubly deprotonated organic ligand **L**, two nitrates, one *o*-vanillin molecule and one methanol molecule. The organic ligand is chelated to the Zn^{II} ion by the two imino N atoms and the two phenoxy O atom. The Y^{III} centre is coordinated to the two methoxy O atom and the two phenoxy O atom belonging to ligand **L**, one phenoxido and one aldehydic oxygen atoms belonging to the *o*-vanillin moiety, two oxygen atoms belonging to one nitrate molecule and one methanol molecule. There is one Zn^{II}-Y^{III} distance at 3.4708(11) Å and the geometry around the Zn^{II} ion can be described as distorted square pyramidal (N_2O_3). The coordination number of the Y^{III} is nine and the coordination geometry can be best described, similarly to **1**, as pentagonal bipyramid (7+2). SHAPE analysis suggests a Muffin geometry (Table S2). Compounds **3** and **4** (Figure 1, c) are isoskeletal, therefore only the crystal structure of **3** will be described. **3** crystallises in the monoclinic *P*2_1/*n* space group. The asymmetric unit contains one Zn^{II} ion, one Dy^{III} ion, one doubly deprotonated organic ligand **L**, two nitrates, one chloride and an ethanol molecule. The organic ligand is chelated to the Zn^{II} ion by the two imino N atoms and the two phenoxy O atom. The Dy^{III} cation on the other hand is coordinated to the two methoxy O atom and the two phenoxy O atom, four oxygen atoms belonging to two nitrates and an ethanol molecule. The geometry of Dy(1) can be best described as pentagonal bipyramid (considering the two O atoms of the two chelated NO_3 units as one). SHAPE analysis suggests a Muffin geometry (Table S2). The distorted square pyramidal geometry (N_2O_2) of the Zn^{II} is completed by a capping chloride anion (Figure 2). The

distance between Ln^{III} and Zn^{II} is 3.4865(7) Å in **3** and 3.4589(6) Å in **4**.

Solution Studies. To determine whether the reported compounds were stable in solution, an electrospray ionisation mass (ESI-MS) spectrometry study was performed. **1** and **2** displayed peaks in the MS (positive-ion mode) which corresponded to the general fragment formula [$Zn^{II}Ln^{III}L(NO_3)_2$]. This indicates that the tetranuclear units of **1** collapse into solution yielding the corresponding dinuclear moiety (Table 2, entries 1 and 2). **3** and **4** displayed peaks in the MS (positive-ion mode) which corresponded to the general fragment formula [$Zn^{II}Dy^{III}LCl(H_2O)_2$]$^+$, indicating that the dinuclear core was retained when solubilised (Table 2, entries 3 and 4).

Table 2. ESI-MS peak assignments for **1**-**4**.

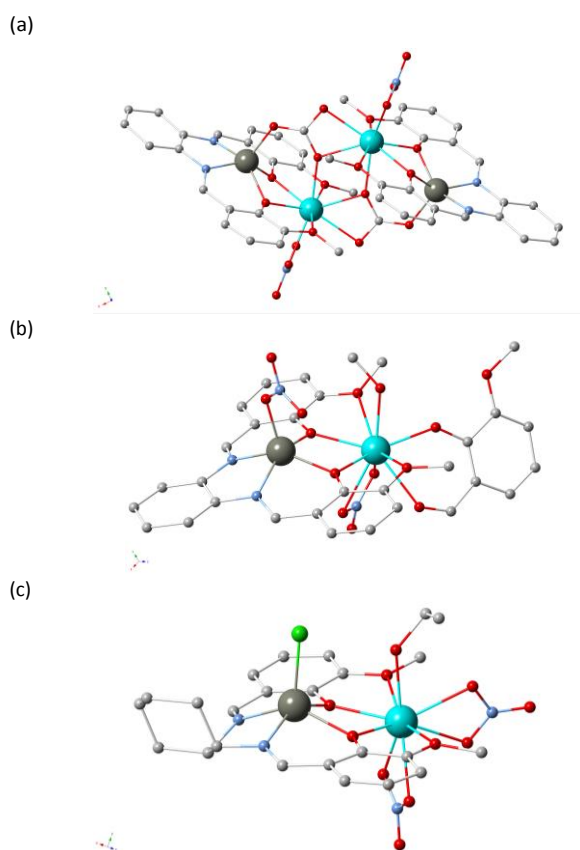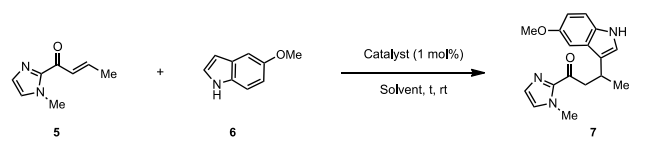| Entry	Compound	Fragment formula	Peak position (m/z)
1	**1**	[$Zn^{II}Dy^{III}(C_{22}H_{24}N_2O_4)(NO_3)_2$]	732.0144
2	**2**	[$Zn^{II}Y^{III}(C_{22}H_{24}N_2O_4)(C_8H_7O_3)(NO_3)$-H]$^+$	746.0396
3	**3**	[$Zn^{II}Dy^{III}(C_{22}H_{24}N_2O_4)Cl(H_2O)_2$-2H]$^+$	677.9702
4	**4**	[$Zn^{II}Y^{III}(C_{22}H_{24}N_2O_4)Cl(H_2O)_2$]$^+$	604.9443

(a)

(b)

(c)

Figure 1. (a) Molecular structure of **1**. Colour code: Dy^{III}-Light blue; Zn^{II}-Grey; O-Red; N-Blue; C-Grey. (b) Molecular Structures of **3**. Colour code: Dy^{III}-Light Blue; Zn^{II}-Grey; O-Red; C-White; N-Pale blue; Cl-Green. (c) Molecular Structures of **4**. Colour code: Dy^{III}-Light Blue; Zn^{II}-Grey; O-Red; C-White; N-Pale blue; Cl-Green. Hydrogen atoms omitted for clarity.

NMR Studies. The NMR spectra of [Zn^{II}Y^{III}L(NO$_3$)$_2$(*o*-van) (MeOH)] in DMSO-d^6 showed one major species with sharp peaks that were easily analysed and consistent with the structure. The cyclohexyldiamino peaks were broadened at room temperature, indicating some degree of mobility with the ring. DOSY measurements gave a D of 2.17 to 2.19e^{-10}, which is consistent with a "mono" nuclear species with MW ~ 500 Da. Looking at the imine proton region, we could see a minor species (5%) with broadened peaks, which 2D NOESY spectra confirmed an exchange with the major form. The low abundance and broadening of these peaks means it is not viable to characterise this species. There are also two other minor species (1.9% and 1.2% each) with sharp peaks, but these did not appear to be exchanging, so it is possible that these are simply impurities. Heating it to 75 °C gave the expected coalescence of the major and minor species, with the other peaks staying the same, consistent with those being impurities. The S/N at room temperature was too small however for an accurate measurement of the diffusion coefficient for the minor species, but it is nonetheless also consistent with a similar molecular weight to the major species.

Table 3. Condition screening.

Entry	Catalyst	Solvent	Time (d)	Yield^a (%)
1	-	MeCN	3	-
2	Cu/dmbpy	MeCN	1	96
3	**1**	MeCN	3	18
4	**1**	MeOH	2	40
5	**1**	EtOAc	4	41
6	**2**	MeOH	5	50
7	**2**	MeCN	3	53
8	**2**	DMF	4	62
9	**2**	Toluene	3	88
10	**2** (1 mol%)	EtOAc	3	99
11	**2** (0.5 mol%)	EtOAc	3	55
12	**2** (0.1 mol%)	EtOAc	3	14
13	**3**	EtOAc	3	90
14	**4**	EtOAc	3	47
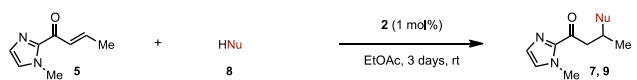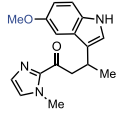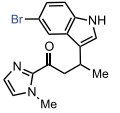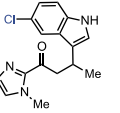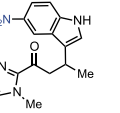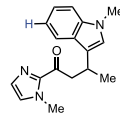
^{a}Isolated yield.

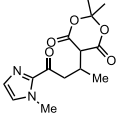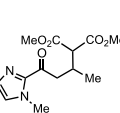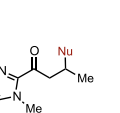**Catalytic Studies.** These CCs were eventually evaluated for their catalytic activity. For the initial benchmarking study, we decided to test the addition of 5-methoxyindole (**6**) to α,β-unsaturated 2-acyl imidazole **5**.[50–53] The reactions were carried at 1.0 mol% loading and the results depicted in Table 3. We first compared the performance of **1** to Copper nitrate/4,4'-dimethyl-2,2'-bipyridine (Cu/dmbpy) (Table 3, entry 2), as this was a common catalytic system used for this kind of transformation. Unfortunately, Cu/dmbpy outcompeted **1** in MeCN (Table 3, entry 2 *vs* 3), while in MeOH the title compound was formed

along with a bi-product which was later identified as the MeO addition product (Table 5, entry 4). The use of a non-nucleophilic solvent such as AcOEt allowed to eliminate any side product formation and afforded the desired Friedel-Crafts product in 41% yield. Substitution of the Dy^{III} ion (**1**) to Y^{III} (**2**) drastically improved the efficacy of the reaction independently of the solvent used (Table 5, entries 6-10), however the best results were obtained in AcOEt as the product was isolated in almost quantitative yield (Table 3, entry 10). Decreasing the catalyst loading from 1.0 mol% to 0.1 mol% reduced the reactivity as the yield dropped to 14% (Table 3, entries 10-12). With these optimised conditions in hand [1.0 mol% catalyst loading, AcOEt, rt], we next compared the catalytic activity of our four catalysts (**1-4**). Interestingly, catalysts **1** and **2** (Table 3, entries 1-12) displayed on average a higher efficacy than the pre-catalysts **3** and **4** (Table 3, entries 13-14). Overall, the Y^{III} compounds showed a higher catalytic activity than the Dy^{III} derivatives, pre-catalyst **2** being the most effective. This may indicate that the efficacy of the CCs is highly dependent on the coordination environment around the Y^{III} and Dy^{III} ions.

Table 4. Reaction scope.

^{a}Isolated yield. ^{b}Reaction run in MeOH.

The scope of the reaction was further investigated with the most efficient CC catalyst **2** using various nucleophiles (Table 4). Unsurprisingly, substitution with electron withdrawing groups on the indole resulted in a substantial reduction in conversion to product (**7b-d**). In contrast, the conjugate addition of *N*-methyl indole was obtained in quantitative yield (**7e**). The method was eventually extended to other type of nucleophiles, particularly 1,3-dioxane-4,6-dione and dimethyl malonate, resulting in the isolation of the respective products **9a** and **9b** in good yields. Finally, our catalytic system was also shown to be compatible with the addition of thiols and alcohols as showcased by the high yields obtained in the formation of the corresponding thioether **9c** (100% yield) and ether **9d** (80% yield). As a general trend, the use of catalysts from the first category may overlook the possible formation of multiple 3d/4f species that may significantly influence the observed catalytic behaviour.

Conclusions

The results presented herein showcase the synthetic challenges revealed during the development of catalytic protocols that involve Zn/4f CCs and the present dinucleating ligand. The present dinucleating Schiff Base ligand represents an ideal candidate for the synthesis of dinuclear 3d/4f catalysts, offering two different pockets for coordination, however unexpected species of different nuclearity can be obtained when different synthetic approaches are followed. The present results notify that in-situ generated catalysts for catalytic screenings is not a good practice as it may overlook the possible formation of multiple 3d/4f species that may influence the observed catalytic behaviour. Our synthetic attempts yielded dinuclear (**2**, **3** and **4**), and tetranuclear (**1**) species that all exist as dinuclear species in solution. All four catalysts were found to promote, probably *via* a cooperative pathway, the addition of indoles on 2-acyl imidazoles as well as the Michael addition of β-diesters in good yields. The catalytic efficacy of the asymmetric version of these catalysts are currently being investigated and will be reported in due course.

Acknowledgements

References

1. G. E. Kostakis, A. M. Ako, and A. K. Powell, *Chem. Soc. Rev.*, 2010, **39**, 2238–2271.
2. C. Papatriantafyllopoulou, E. E. Moushi, G. Christou, and A. J. Tasiopoulos, *Chem. Soc. Rev.*, 2016, **45**, 1597–1628.
3. P. Abbasi, K. Quinn, D. I. Alexandropoulos, M. Damjanović, W. Wernsdorfer, A. Escuer, J. Mayans, M. Pilkington, and T. C. Stamatatos, *J. Am. Chem. Soc.*, 2017, **139**, 15644–15647.
4. J. Wu, X.-L. Li, M. Guo, L. Zhao, Y.-Q. Zhang, and J. Tang, *Chem. Commun.*, 2018, **54**, 1065–1068.
5. J. Long, J. Rouquette, J.-M. Thibaud, R. A. S. Ferreira, L. D. Carlos, B. Donnadieu, V. Vieru, L. F. Chibotaru, L. Konczewicz, J. Haines, Y. Guari, and J. Larionova, *Angew. Chem. Int. Ed.*, 2015, **54**, 2236–2240.
6. M. Ostrowska, I. O. Fritsky, E. Gumienna-Kontecka, and A. V Pavlishchuk, *Coord. Chem. Rev.*, 2016, **327–328**, 304–332.
7. D. I. Alexandropoulos, L. Cunha-Silva, G. Lorusso, M. Evangelisti, J. Tang, and T. C. Stamatatos, *Chem. Commun.*, 2016, **52**, 1693–1696.
8. B. Berkoff, K. Griffiths, A. Abdul-Sada, G. J. Tizzard, S. J. Coles, A. Escuer, and G. E. Kostakis, *Dalton Trans.*, 2015, **44**, 12788–12795.
9. J.-B. Peng, X.-J. Kong, Q.-C. Zhang, M. Orendáč, J. Prokleška, Y.-P. Ren, L.-S. Long, Z. Zheng, and L.-S. Zheng, *J. Am. Chem. Soc.*, 2014, **136**, 17938–17941.
10. J. Wu, L. Zhao, L. Zhang, X.-L. Li, M. Guo, A. K. Powell, and J. Tang, *Angew. Chemie Int. Ed.*, 2016, **55**, 15574–15578.
11. L. Zhao, J. Wu, H. Ke, and J. Tang, *Inorg. Chem.*, 2014, **53**, 3519–3525.
12. J.-H. Xu, L.-Y. Guo, H.-F. Su, X. Gao, X.-F. Wu, W.-G. Wang, C.-H. Tung, and D. Sun, *Inorg. Chem.*, 2017, **56**, 1591–1598.
13. B. M. Trost, J. Jaratjaroonphong, and V. Reutrakul, *J. Am. Chem. Soc.*, 2006, **128**, 2778–2779.
14. A. A. Opalade, A. Karmakar, G. M. D. M. Rúbio, A. J. L. Pombeiro, and N. Gerasimchuk, *Inorg. Chem.*, 2017, **56**, 13962–13974.
15. S. Kato, M. Kanai, and S. Matsunaga, *Chem. – An Asian J.*, 2013, **8**, 1768–1771.
16. E. F. DiMauro and M. C. Kozlowski, *Organometallics*, 2002, **21**, 1454–1461.
17. P. Mahapatra, M. G. B. Drew, and A. Ghosh, *Cryst. Growth Des.*, 2017, **17**, 6809–6820.
18. S. Handa, K. Nagawa, Y. Sohtome, S. Matsunaga, and M. Shibasaki, *Angew. Chem. Int. Ed.*, 2008, **47**, 3230–3233.
19. D. S. Nesterov, E. N. Chygorin, V. N. Kokozay, V. V. Bon, R. Boča, Y. N. Kozlov, L. S. Shul'pina, J. Jezierska, A. Ozarowski, A. J. L. Pombeiro, and G. B. Shul'pin, *Inorg. Chem.*, 2012, **51**, 9110–9122.
20. S. Handa, V. Gnanadesikan, S. Matsunaga, and M. Shibasaki, *J. Am. Chem. Soc.*, 2007, **129**, 4900–4901.
21. S. Handa, V. Gnanadesikan, S. Matsunaga, and M. Shibasaki, *J. Am. Chem. Soc.*, 2010, **132**, 4925–4934.
22. Y. Li, P. Deng, Y. Zeng, Y. Xiong, and H. Zhou, *Org. Lett.*, 2016, **18**, 1578–1581.
23. M. Furutachi, S. Mouri, S. Matsunaga, and M. Shibasaki, *Chem. – An Asian J.*, 2010, **5**, 2351–2354.
24. F. Evangelisti, R. Moré, F. Hodel, S. Luber, and G. R. Patzke, *J. Am. Chem. Soc.*, 2015, **137**, 11076–11084.
25. G. Maayan and G. Christou, *Inorg. Chem.*, 2011, **50**, 7015–7021.
26. K. Griffiths, P. Kumar, G. Akien, N. F. Chilton, A. Abdul-Sada, G. J. Tizzard, S. Coles, and G. E. Kostakis, *Chem. Commun.*, 2016, **52**, 7866–7869.
27. P. Kumar, K. Griffiths, S. Lymperopoulou, and G. E. Kostakis, *RSC Adv.*, 2016, **6**, 79180–79184.
28. K. Griffiths, P. Kumar, J. D. Mattock, A. Abdul-Sada, M. B. Pitak, S. J. Coles, O. Navarro, A. Vargas, and G. E. Kostakis, *Inorg. Chem.*, 2016, **55**, 6988–6994.
29. K. Griffiths, A. C. Tsipis, P. Kumar, O. P. E. Townrow, A. Abdul-Sada, G. R. Akien, A. Baldansuren, A. C. Spivey, and G. E. Kostakis, *Inorg. Chem.*, 2017, **56**, 9563–9573.
30. Q. Shi, X. Yang, X. Zhang, X. Li, J. Yang, and X. Lü, *Inorg. Chem. Commun.*, 2016, **73**, 4–6.
31. A. Draksharapu, W. Rasheed, J. E. M. N. Klein, and L. Que, *Angew. Chemie Int. Ed.*, 2017, **56**, 9091–9095.
32. K. Griffiths, C. W. D. Gallop, A. Abdul-Sada, A. Vargas, O. Navarro, and G. E. Kostakis, *Chem. Eur. J.*, 2015, **21**, 6358–6361.
33. L. Wang, C. Xu, Q. Han, X. Tang, P. Zhou, R. Zhang, G. Gao, B. Xu, W. Qin, and W. Liu, *Chem. Commun.*, 2018, DOI:10.1039/C7CC09092G.
34. H. Feng, Z. Zhang, W. Feng, P. Su, X. Lü, D. Fan, W.-K. Wong, R. A. Jones, and C. Su, *Inorg. Chem. Commun.*, 2014, **43**, 151–154.
35. S. J. Coles and P. A. Gale, *Chem. Sci.*, 2012, **3**, 683–689.
36. G. M. Sheldrick, *Acta Crystallogr. Sect. C Struct. Chem.*, 2015, **71**, 3–8.
37. A. L. Spek, *J. Appl. Crystallogr.*, 2003, **36**, 7–13.
38. O. V. Dolomanov, L. J. Bourhis, R. J. Gildea, J. A. K. Howard, and H. Puschmann, *J. Appl. Crystallogr.*, 2009, **42**, 339–341.
39. L. J. Farrugia, *J. Appl. Crystallogr.*, 2012, **45**, 849–854.
40. C. F. Macrae, P. R. Edgington, P. McCabe, E. Pidcock, G. P. Shields, R. Taylor, M. Towler, and J. Van De Streek, *J. Appl. Crystallogr.*, 2006, **39**, 453–457.
41. P. Zhang, L. Zhang, S. Lin, and J. Tang, *Inorg. Chem.*, 2013, **52**, 6595–6602.
42. L. Liu, Z. Zhang, W. Feng, C. Yu, X. Lü, W.-K. Wong, and R. A. Jones, *Inorg. Chem. Commun.*, 2014, **49**, 124–126.
43. T. Gao, L. L. Xu, Q. Zhang, G. M. Li, and P. F. Yan, *Inorg. Chem. Commun.*, 2012, **26**, 60–63.
44. Y. Zhang, W. Feng, H. Liu, Z. Zhang, X. Lü, J. Song, D. Fan, W. K. Wong, and R. A. Jones, *Inorg. Chem. Commun.*, 2012, **24**, 148–152.
45. W. X. Feng, Y. N. Hui, G. X. Shi, D. Zou, X. Q. Lü, J. R. Song, D. Di Fan, W. K. Wong, and R. A. Jones, *Inorg. Chem. Commun.*, 2012, **20**, 33–36.
46. T. Miao, Z. Zhang, W. Feng, P. Su, H. Feng, X. Lü, D. Fan, W. K. Wong, R. A. Jones, and C. Su, *Spectrochim. Acta - Part A Mol. Biomol. Spectrosc.*, 2014, **132**, 205–214.
47. Y.-M. Tian, H.-F. Li, B.-L. Han, Q. Zhang, and W.-B. Sun, *Acta Crystallogr. Sect. E Struct. Reports Online*, 2012, **68**, m1500–

m1501.

48. W.-B. Sun, P.-F. Yan, S.-D. Jiang, B.-W. Wang, Y.-Q. Zhang, H.-F. Li, P. Chen, Z.-M. Wang, and S. Gao, *Chem. Sci.*, 2016, **7**, 684–691.

49. M. Llunell, D. Casanova, J. Cirera, P. Alemany, S. Alvarez, and SHAPE: Program for the Stereochemical Analysis of Molecular Fragments by Means of Continuous Shape Measures and Assosciated Tools, Version 2.1, Barcelona, 2013.

50. K. Amirbekyan, N. Duchemin, E. Benedetti, R. Joseph, A. Colon, S. A. Markarian, L. Bethge, S. Vonhoff, S. Klussmann, J. Cossy, J. J. Vasseur, S. Arseniyadis, and M. Smietana, *ACS Catal.*, 2016, **6**, 3096–3105.

51. N. Duchemin, I. Heath-Apostolopoulos, M. Smietana, and S. Arseniyadis, *Org. Biomol. Chem.*, 2017, **15**, 7072–7087.

52. N. Duchemin, E. Benedetti, L. Bethge, S. Vonhoff, S. Klussmann, J.-J. Vasseur, J. Cossy, M. Smietana, and S. Arseniyadis, *Chem. Commun.*, 2016, **52**, 8604–8607.

53. E. Benedetti, N. Duchemin, L. Bethge, S. Vonhoff, S. Klussmann, J.-J. Vasseur, J. Cossy, M. Smietana, and S. Arseniyadis, *Chem. Commun.*, 2015, **51**, 6076–6079.